Interaction of α-Crystallin with Spin-Labeled Peptides†

Zohreh Toossi Farahbakhsh,‡ Qing-Ling Huang,‡ Lin-Lin Ding,‡ Christian Altenbach,‡ Heinz-Jürgen Steinhoff,§ Joseph Horwitz,*,‡ and Wayne L. Hubbell*,‡,||

Jules Stein Eye Institute and Department of Chemistry and Biochemistry, University of California, Los Angeles, California 90024-7008, and Institut für Biophysik, Ruhr-Universität Bochum, Universitätsstrasse 150, W-44780 Bochum, Germany

Received July 28, 1994; Revised Manuscript Received November 1, 1994⊗

ABSTRACT: α-Crystallin is a major protein of the vertebrate lens once thought to be highly specialized for conferring transparency. However, recent work has revealed a wide tissue distribution and a sequence homology to small heat shock proteins, suggesting a more general role for the protein. Like other molecular chaperons, α-crystallin is known to bind to unfolded proteins and suppress nonspecific aggregation *in vitro*. In the present work, spin-labeled derivatives of the insulin B chain and melittin were used to investigate the state of these proteins bound to α-crystallin. Insulin was selected since unfolding can be triggered by reduction of the interchain disulfide bonds, a treatment that does not affect α-crystallin. Upon reduction of insulin, the separated B chains aggregate. In the presence of α-crystallin, the B chains bind to α-crystallin and aggregation is suppressed. Melittin, a 26 amino acid peptide from bee venom, was selected for study since it is a random coil under physiological conditions, and its interaction with α-crystallin can be directly studied. EPR analysis of the spin-labeled peptides shows that the nitroxide side chains are immobilized in a polar environment on α-crystallin and that they are separated by 25 Å or more in the complex, indicating that the bound proteins are not clustered. The bound B chains of insulin are not in a fully extended conformation, and melittin does not appear to bind to a hydrophobic surface in α-crystallin as an amphipathic helix, as it does to membranes and some other proteins. Equilibrium binding studies for melittin give a stoichiometry of approximately 1:1 melittin/α-crystallin monomer, with a dissociation constant of 7.3 μM.

α-Crystallin is one of the major proteins of the lens and is considered to be responsible for its stability and refractive properties (Bloemendal, 1981; Wistow & Piatigorsky, 1988; Bloemendal & de Jong, 1991; Piatigorsky, 1992). It is a water-soluble protein with an average molecular mass of 800 kDa (Bloemendal, 1981; Harding & Crabbe, 1984; Augusteyn et al., 1992) and is composed of two homologous subunits, αA and αB, of approximately 20 kDa each (Overbeek et al., 1985; Chepelinsky et al., 1985). Until the mid 1980's, it was thought that these subunits are strictly lens-specific. However, it is now clear that both subunits are expressed in nonlenticular tissues as well. αB-Crystallin has been found in tissues such as heart, skeletal muscle, skin, brain, spinal cord, and lung (Bhat et al., 1988; Bhat & Nagineni, 1989; Dubin et al., 1989). Recently, with more sensitive immunochemical techniques, αA-crystallin was also detected in non-lens tissues, with the highest concentration being in the spleen and thymus (Kato et al., 1991). Increased expression of α-crystallin has been found in various neurological diseases such as Alexander's disease and Lewy body disease (Iwaki et al., 1989; Lowe et al., 1990) and under heat and hypertonic stress (Klemenz et al., 1991; Dasgupta et al., 1992; Inaguma et al., 1992). The function of α-crystallin in nonlenticular tissues is unknown, although it has been shown that α-crystallins are related by sequence to the small heat shock proteins (Ingolia & Graig, 1982; Nene et al., 1986). α-Crystallins and small heat shock proteins share some important properties, including the formation of large assemblies (Bindels et al., 1979; Tardieu et al., 1986; Augusteyn & Koretz, 1987; Walsh et al., 1991), stress inducibility, intracellular relocalization (Klemenz et al., 1991), autophosphorylation (Kantrow & Piatigorsky, 1994), phosphorylation after stress (Gaestel et al., 1991; Landry et al., 1992), and interaction with plasma membranes (Mulders et al., 1989; Adamska, 1991) or cytoskeletal elements (Bloemendal et al., 1984; Miron et al., 1991). Recent *in vitro* experiments have shown that mouse HSP25, as well as αA- and αB-crystallin, can act as molecular chaperons (Nicholl & Quinlan, 1994; Jakob et al., 1993; Horwitz, 1992; Merck et al., 1993; Rao et al., 1994). These findings suggest a possible chaperon role for α-crystallin *in vivo* as well (Jakob & Buchner, 1994).

The purpose of the present work is to characterize the interaction of unfolded proteins with α-crystallin. In previous studies with a similar goal, the protein under study was denatured with heat or chaotropic agents in the presence of α-crystallin (Rao et al., 1993; Boyle et al., 1993). Under these conditions α-crystallin itself may be affected by the denaturant, thus complicating interpretation of results. In the present work, this problem is overcome by using insulin, which can be unfolded by reducing the interchain disulfide bonds, and melittin, a random coil under physiological conditions.

† Research reported here was supported by NIH Grants EY05216 (W.L.H.), EY3897 (J.H.), the Max Kade Foundation (H.J.S.), Research to Prevent Blindness (W.L.H. and J.H.), and the Jules Stein Professor endowment (W.L.H.).

* Address correspondence to these authors.
‡ Jules Stein Eye Institute, UCLA.
§ Ruhr-Universität Bochum.
|| Department of Chemistry and Biochemistry, UCLA.

⊗ Abstract published in *Advance ACS Abstracts*, December 15, 1994.

0006-2960/95/0434-509$09.00/0

Scheme 1

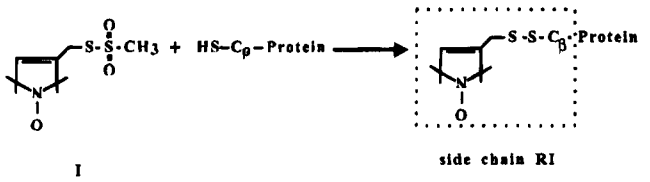

I

Scheme 2

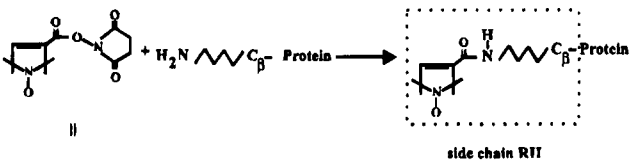

II

MATERIALS AND METHODS

Materials

Insulin and insulin derivatized at the amino terminus of insulin B chain with fluorescein isothiocyanate (FITC[1]-insulin) were obtained from Sigma. α-Crystallin was purified as described previously (Horwitz, 1992). The methanethiosulfonate spin label, *S*-(1-oxy-2,2,5,5-tetramethylpyrroline-3-methyl)methanethiosulfonate, hereafter referred to as spin label I, was a gift of Kalman Hideg (University of Pécs, Pécs, Hungary). Succinimidyl 2,2,5,5-tetramethyl-3-pyrroline-1-oxyl-3-carboxylate, hereafter referred to as spin label II, was obtained from Molecular Probes (Eugene, OR).

Methods

Light Scattering Assay for B Chain Aggregation and Preparation of the α-Crystallin/B Chain Complex. To assay for aggregation, 0.1 mg of insulin was reduced with 20 mM dithiothreitol in the presence of variable amounts of α-crystallin at 25 °C in a final volume of 0.4 mL. Aggregation of the insulin B chain was monitored by measuring the apparent absorption due to scattering at 360 nm in a Beckman Du 70 spectrophotometer with a 10-mm path length.

To prepare the α-crystallin/B chain complex, 0.5 mg of insulin was reduced with 20 mM DTT at 25 °C in the presence of 3 mg of α-crystallin in a final volume of 0.5 mL. The complex was then separated from the soluble A chain and excess reducing reagent by gel filtration chromatography on a HR-6 column (Pharmacia) at a flow rate of 0.5 mL/min. The elution buffer was 20 mM Tris and 0.1 M NaCl, pH 7.9. The crystallin−B-chain complex fraction eluting at 18−28 min was collected and used for reaction with spin label I.

Spin Labeling of Insulin at Cysteine Residues. Cysteine residues C7 and C19 of the insulin B chain in the α-crystallin−B-chain complex were modified with spin label I to yield the spin-labeled side chain RI (Scheme 1). Spin-labeled peptides will be identified by specifying the peptide, the side chain, and the sequence position. For example, insulin B RI(7,19) denotes the insulin B chain with side chain RI at positions 7 and 19.

To achieve specific labeling of the insulin cysteine residues in the complex, the single cysteine residue of αA-crystallin was blocked by carboxymethylation according to the following procedure: 35 mg of α-crystallin was dissolved in 0.55 mL of 20 mM Tris-HCl, pH 7.4, containing 0.1 M NaCl and 5 M urea to unfold the protein and fully expose the sulfhydryl groups to modification. The solution was incubated for 1 h at room temperature after which 19 mg of iodoacetate in 0.59 mL of 0.1 M Tris buffer, pH 8.0, was added. The reaction mixture was incubated for 30 min in the dark at room temperature after which it was exhaustively dialyzed against 50 mM sodium phosphate buffer and 0.1 M NaCl, pH 7.0 (PBS buffer), to remove urea and refold the protein (Thomson & Augusteyn, 1984). The carboxymethylation did not affect the structure or properties of refolded α-crystallin as judged by circular dichroism and binding of the insulin B chain. The carboxymethylated α-crystallin (CM-α-crystallin) was used for the preparation of the complex as described above. To label the cysteine residues of the bound insulin B chain, a 10 μM solution of the complex was incubated with a 5-fold molar excess of the spin label I for 16 h at 25 °C. The unreacted spin label was removed by repeated washing of the labeled protein in a Centricon 30 microconcentrator (Amicon).

Aggregated insulin B chain was prepared by incubation of 1 mg of insulin in 0.5 mL of PBS buffer, containing 20 mM DTT for 2 h at 25 °C. The aggregated B chain was washed with PBS buffer several times to remove DTT and the soluble A chain. The pellet was solubilized in 1% SDS, and a 5-fold molar excess spin label I was added and the mixture incubated for 16 h at 25 °C. The mixture was dialyzed against PBS buffer for 2 days with several buffer changes to remove the SDS and unreacted spin label. After removal of SDS the B chain precipitate was recovered by centrifugation, resuspended in a small volume of the buffer, and the EPR spectrum recorded.

Spin Labeling of FITC-Insulin at Lysine-29. The B chain α-amino group of FITC insulin is blocked by the fluorescein isothiocyanate group, and the single reactive lysine in the B chain (K29) can be derivatized with spin label II to yield spin-labeled side chain RII (Scheme 2). The reaction is carried out at 25 °C in PBS buffer, pH 8.0, for 3 h with a final FITC-insulin concentration of 0.6 mM and a 10-fold molar excess of spin label. The unreacted spin label was removed by washing the labeled protein in Centricon 3 microconcentrator. The labeled insulin was then used for preparation of the α-crystallin−B-chain complex as described above.

Spin-Labeled Melittin Derivatives. Spin-labeled melittin derivatized with side chain RII at positions 7, 21, or 23 was prepared as previously described (Altenbach & Hubbell, 1988). To determine the binding constant and stoichiometry for the equilibrium interaction of melittin and α-crystallin, an EPR spectrum of a known concentration of free melittin in solution was subtracted from the composite spectrum of an equilibrium mixture of melittin and α-crystallin. The composite spectrum contains both bound (immobilized) and free (mobile) components, and the subtraction endpoint was conveniently judged by the disappearance of the mobile component. The fraction of the free reference spectrum needed to reach the endpoint gave the free melittin concentration and, by difference from the total amount of melittin, the bound melittin concentration. The concentration of α-crystallin in the sample was determined by measuring the

[1] Abbreviations: FITC, fluorescein isothiocyanate; DTT, dithiothreitol; CM-α-crystallin, *S*-carboxymethylated α-crystallin; TEMPOL, 2,2,6,6-tetramethyl,4-hydroxy-1-piperidinyloxy.

absorbance at 280 nm using an extinction coefficient of $E^{280}_{0.01\%} = 0.8$ cm^{-1}. From the above information, the stoichiometry and binding constant can be estimated by Scatchard analysis.

EPR Measurements. EPR spectra were recorded at X-band with a Varian E-109 spectrometer fitted with a loop-gap resonator (Hubbell et al., 1987) and interfaced to a Nicolet 1280 computer (Nicolet Instrument Corporation, Madison, WI). Spin label concentrations were determined by double integration of the EPR spectra and comparison with a standard solution of TEMPOL. Collision rates of spin-labels with O_2 in air equilibrium solution were estimated using the power saturation technique as previously described (Altenbach et al., 1994). Saturation data were analyzed in terms of the dimensionless parameter Π, which provides an instrument- and line-shape-independent measure of the collision frequency (Farahbakhsh et al., 1992).

Estimation of Interspin Distance in Spin Labeled Proteins. If two immobilized spin labels are at fixed positions in a protein, dipolar interactions between the spins may lead to detectable effects on the EPR spectrum. To analyze such interactions free from dynamic effects, spectra are recorded in a frozen state. For an isotropic distribution of interspin vectors at a distance between about 10 and 25 Å, the effect is a general broadening of the resonance lines, and the degree of broadening can be used to estimate the interspin distance. A computer fitting procedure (Steinhoff et al. 1991; Steinhoff, 1988) was used to determine the interspin distance from such broadened spectra. In the simulation, the distribution of molecular orientations of the spin labels with respect to each other and the distribution of the distance vector between interacting spin labels with respect to the magnetic field is taken to be isotropic. To allow for a range of distances expected to arise from a distribution of conformations of either the protein or the spin label side chain, a Gaussian distribution of interspin distances with an average distance $\langle r \rangle$ and width σ is permitted. To reduce the number of fit parameters, the values of the magnetic tensor parameters A_{xx}, A_{yy}, g_{xx}, g_{yy}, and g_{zz} were obtained by fitting powder spectra obtained at 183 K from samples of bacteriorhodopsin with side chain RI at either position 103 or 127 (Altenbach et al., 1994) where dipolar interactions could be excluded. Spectra of labeled α-crystallin in 20% glycerol were recorded at 183 K at a microwave power of 50 μW to minimize saturation effects. The spectra were fit with A_{zz}, $\langle r \rangle$, and σ as adjustable parameters. A_{zz} was varied to account for differences in polarity of the spin label environments.

RESULTS

α-Crystallin Prevents the Aggregation of the Insulin B Chain. Reduction of the insulin interchain disulfides leads to aggregation and precipitation of the B chain while the A chain remains in solution (Sanger, 1949). The aggregation can be monitored by measuring the apparent absorbance due to light scattering at 360 nm as shown in Figure 1, curve 1. The ability of α-crystallin to protect insulin B chain from aggregation was tested by reducing insulin at various ratios of insulin/α-crystallin. As shown in Figure 1, curves 2−4, the addition of α-crystallin significantly delays the onset of the B chain aggregation, reduces the rate of aggregation, and reduces the final value of the scattering. As shown by curve 4, a weight ratio of insulin/α-crystallin of 1:6 is sufficient

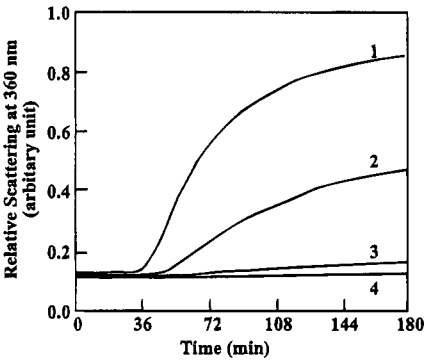

FIGURE 1: Aggregation of insulin after reduction by dithiothreitol in the absence and presence of α-crystallin. The incubation mixture contained, in a final volume of 0.4 mL, 50 mM sodium phosphate, 100 mM NaCl, pH 7.0, 0.1 mg of insulin, and 20 mM DTT with the following additions: curve 1, none; curve 2, 0.2 mg of α-crystallin; curve 3, 0.6 mg; curve 4, 1 mg. The path length was 10 mm.

for complete protection of the B chain from aggregation. Taking the molecular mass of the α-crystallin monomer to be 20 kDa and that of insulin B chain as 3 kDa, this corresponds to a stoichiometry of approximately one molecule of B chain per 1.7 mol of α-crystallin monomer.

α-Crystallin Forms a Stable Complex with the Insulin B Chain. The interaction of α-crystallin with the insulin B chain was investigated by size exclusion chromatography using FITC-insulin. Under nondenaturing conditions, a mixture of α-crystallin and FITC-insulin are completely separable when chromatographed on a size exclusion column as shown by the profile in Figure 2a. The intense peak at 41 min absorbing at 495 nm is due to free FITC in the commercial insulin preparation. Either α-crystallin or FITC insulin alone elute at the corresponding times indicated in Figure 2a . If FITC insulin is reduced with DTT in the presence of α-crystallin, the B chain co-elutes with α-crystallin, as shown by the 495-nm absorbance of the FITC chromophore bound to the B chain (Figure 2b). This demonstrates the formation of a stable complex between α-crystallin and the B chain.

Characterization of the Insulin B Chain in the α-Crystallin/B Chain Complex. In order to characterize the insulin B chain and its environment in the complex, the cysteine residues C7 and C19 of the insulin B chain bound to CM-α-crystallin were modified with spin label I to yield 1.9 spins/insulin. In CM-α-crystallin, the single reactive cysteine on αA-crystallin itself is blocked by more than 99%.

The nature of the binding site in the complex is reflected in part by the polarity of the local environment of the nitroxides. The isotropic hyperfine coupling constants (A_N) of nitroxides are linearly related to solvent polarity as measured, for example, by the Kosower Z factor (Knauer & Napier, 1976). A_N is in turn linearly related to A_{zz}, an element of the hyperfine coupling tensor (Griffith et al., 1974), and A_{zz} can thus be used as a measure of polarity around the nitroxide. In the absence of motion at low temperature, A_{zz} can be determined directly from the maximum splitting in the EPR spectrum (Figure 3a). For the pyrrolidine nitroxides used in all of this studies, A_{zz} ranges from 33 Gauss in CCl_4 (nonpolar) to 35.7 Gauss in water (polar) (Windle, 1981). A similar range of values is found for the side chain RI in bacteriorhodopsin (bR) (Altenbach et al., 1994). For example, A_{zz} is 33 Gauss for bR RI(113) in contact with the

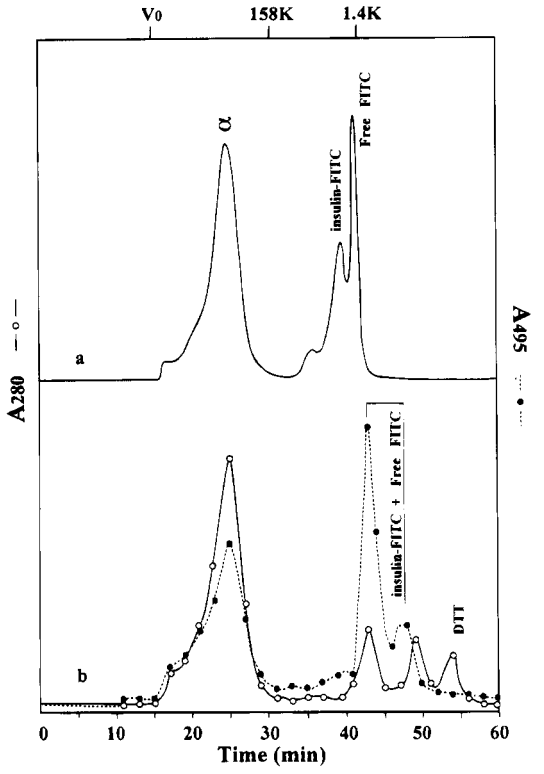

FIGURE 2: Chromatographic profile of a mixture of α-crystallin and FITC-insulin under native and reduced conditions. The mixture was chromatographed on a Pharmacia HR-6 column as described under Methods. The top chromatogram represents a mixture of α-crystallin FITC-insulin (6:1 w/w) under native conditions. The commercial FITC-insulin is prepared according to Teize et al. (1962) and contains unreacted FITC. The bottom chromatogram represents the same mixture after reduction with DTT. The insulin B chain was detected by the absorbance at 495 nm due to the FITC moiety.

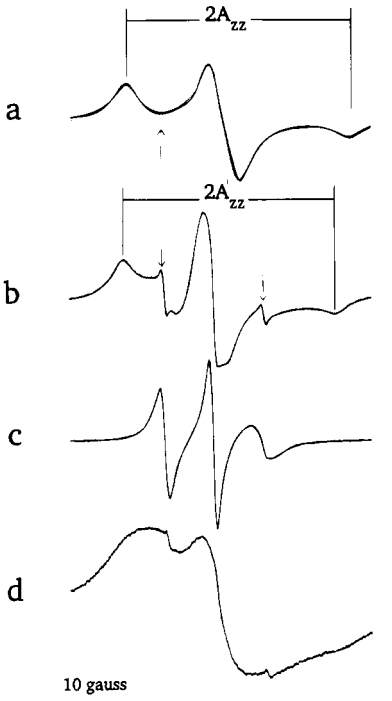

FIGURE 3: EPR spectra of insulin B RI(7,19). (a) Bound to α-crystallin at 183 K; (b) bound to α-crystallin at room temperature. The low amplitude sharp signal (arrows) is due to a small amount of unattached spin label (I) in solution. (c) The sample from spectrum b in 0.5% SDS. (d) Aggregated B chain in the absence of α-crystallin at room temperature.

nonpolar hydrocarbon chains of the bilayer and 36 Gauss for bR RI(103) in the aqueous phase. Sites known to be buried within the apolar interior of the protein colicin E1 have values of A_{zz} in the range of 33−34 Gauss, consistent with values from apolar solvents (L. Salwinski & W. L. Hubbell, unpublished). The A_{zz} values for the spin-labeled proteins complexed with α-crystallin reported here are given in Table 1. For insulin B RI(7,19) bound to crystallin, A_{zz} is 35.4 Gauss, indicating that the nitroxides are in a relatively polar environment, similar to water.

The EPR line shape of insulin B RI(7,19) at room temperature (Figure 3b) is characteristic of a nitroxide in the slow motional limit, i.e., "immobilized" (Schneider & Freed, 1989). The rotational correlation time (τ) is approximately 50 ns as computed from A_{zz}' (Figure 3b) and the corresponding rigid limit value A_{zz} according to the method of Goldman et al. (1972) (see Table 1 for values). When the labeled complex was denatured with 0.5% SDS, the nitroxide becomes very mobile with a correlation time of 1−2 ns, demonstrating the dissociation of the complex (Figure 3c).

Further information regarding the environment of spin-labeled side chains in the complex can be obtained from the accessibility of the nitroxides to collision with O_2. Accessibilities are expressed in terms of a dimensionless parameter Π proportional to the collision frequency (Farahbakhsh et al., 1992; Resek et al., 1993). For the spin labels on the B chain bound to α-crystallin, $\Pi(O_2) = 0.05$. For reference,

Table 1: Nitroxide A_{zz}, A_{zz}' and Correlation Times

Protein	A_{zz}' (α)[a]	A_{zz} (α)[b]	A_{zz} (H_2O)[c]	τ[d]
Insulin B RI(7,19)	34.4	35.4		50
Insulin B RII29	33.8	35.4		30
Melittin RII7	33.8	35.4	35.9	30
Melittin RII21	33.8	35.4	35.9	30
Melittin RII23	33.8	35.4	35.9	30

[a]Values in Gauss for peptides bound to α-crystallin at room temperature. [b]Rigid limit values in Gauss for peptides bound to α-crystallin in 20% glycerol−water at 183 K. [c]Rigid limit values in Gauss for peptides in 20% glycerol−water at 183 K. [d]Approximate correlation times in nanoseconds.

$\Pi(O_2)$ values range from 0 to 0.04 for sites buried in a protein interior to 0.3 for mobile, solvent-accessible surface sites (Hubbell & Altenbach, 1994; L. Salwinski & W. L. Hubbell, unpublished). By this criterion, the sites on insulin are in a relatively inaccessible environment, consistent with the immobilized EPR lineshape.

As shown by light scattering (Figure 1), reduction of the insulin in the absence of α-crystallin is accompanied by aggregation of the B chain. Figure 3d shows the room temperature EPR spectrum of an aggregated state for the spin-labeled B chain. The single broad resonance line is indicative of strong dipolar and/or exchange interaction between the spin labels. This strong spin−spin interaction is characteristic of a configuration where the nitroxides can closely approach one another, such as in a nonspecific aggregate. Comparison of this spectrum with that in Figure 3b provides a convincing argument that the B chains on the α-crystallin molecule are not present in an aggregated state, either in a central cavity in the α-crystallin oligomer or on a binding surface.

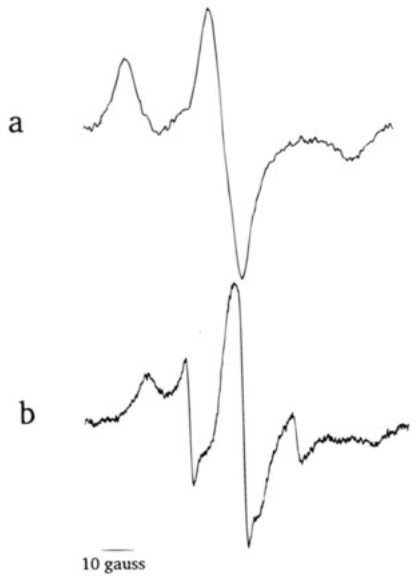

FIGURE 4: EPR spectra of insulin B RII29. (a) Bound to α-crystallin at 183 K; (b) bound to α-crystallin at room temperature.

Each B chain bound to α-crystallin contains two spin labels. If they are ≤25 Å apart in the complex, it should be possible to detect spin−spin interactions between them as a broadening of the lines in the EPR spectrum. Broadening is indeed evident in Figure 3b, where spectral intensity extends over ≈100 Gauss. Quantitative analysis of the interaction in terms of interspin distance must be carried out in the absence of motion. In these studies, dynamic effects are eliminated by freezing the sample. Figure 3a shows the EPR spectrum of the B chain labeled at C7 and C19 bound to α-crystallin at 183 K. Qualitatively, line broadening due to dipolar interaction is evident in this spectrum as judged by the fact that the first derivative resonance intensity does not return to baseline between the low and midfield resonances (arrow in Figure 3a) as it does for noninteracting spins under the same conditions (Figure 6e and discussion below). The least-squares best fit to the spectrum using the dipolar interaction model described under Methods gives an average interspin distance of $\langle r \rangle = 18$ Å with $\sigma = 6$ Å. The fit is excellent, as shown by the thin trace in Figure 3a.

The dipolar interaction discussed above may contain contributions from interactions between spin labels on adjacent B chains in the complex as well as from interactions between the two nitroxides within a single B chain. In order to distinguish these cases, a complex with a molar stoichiometry of 1:8.5 B chain/α-crystallin monomer was prepared. At this dilution, the interchain spin interactions should be undetectable. The EPR spectrum in a frozen glass was very similar to that in the 1:1.7 complex and gave an average interspin distance of $\langle r \rangle = 20$ Å with $\sigma = 5$ Å (data not shown). Thus, the observed interaction may contain a small intermolecular contribution but is dominated by intramolecular interactions.

The EPR spectra of insulin B RII29 bound to α-crystallin at 183 K and room temperature are shown in Figure 4, spectra a and b, and the values of A_{zz}, A_{zz}', and τ are given in Table 1. As for the RI side chains at 7 and 19, the nitroxide in this derivative is in a polar environment and in an immobilized state. The low temperature spectrum shows no evidence of dipolar interaction between bound spins. However, this result does not allow a conclusion to be reached regarding the probable distance between B chains in the complex, since the preparation of the complex requires the use of DTT, resulting in partial reduction of the nitroxides to a diamagnetic state.

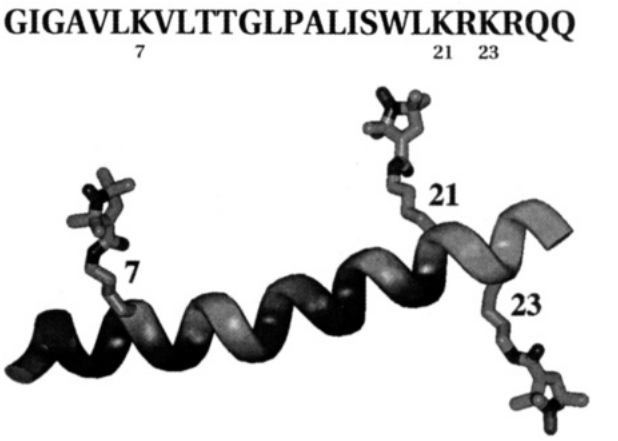

FIGURE 5: Sequence and helical conformation of spin-labeled melittin. (a) The amino acid sequence of melittin with the spin labeled sites indicated. (b) The helical conformation of the melittin monomer, showing the structure of the RII side chains at the positions studied. The positions of hydrophobic residues are indicated with dark shading on the backbone.

Spin-Labeled Melittin Binds to α-Crystallin. Melittin is a 26-amino acid peptide from bee venom that is a random coil at physiological ionic strength and pH, but at high ionic strength electrostatic repulsions are screened, and tetramers are formed (Wilcox & Eisenberg, 1992). Each monomer is an amphipathic α-helix, and the tetramer is stabilized by hydrophobic interactions between the four helices (Terwilliger & Eisenberg, 1982). In the present work, spin-labeled derivatives of melittin with side chain RII at positions 7, 21, or 23 are utilized to investigate the binding of melittin to α-crystallin and its structure in the bound state. The sequence of melittin with the labeled positions indicated is shown in Figure 5.

Figure 6 shows EPR spectra of a constant amount of melittin RII21 in the presence of increasing quantities of α-crystallin. In solution, the spectrum of melittin RII21 alone is characteristic of a highly mobile nitroxide (Figure 6a). This is expected for a nitroxide attached to the flexible lysine side chain in a peptide with a random coil configuration. In the presence of increasing amounts of α-crystallin, an immobilized component grows at the expense of the mobile component arising from free melittin in solution (Figures 6b−d). This reflects the equilibrium binding of melittin to α-crystallin, and the amount of bound and free melittin can be directly determined from the spectra as described under Methods. An analysis of such data is shown in Figure 7 and suggests a single binding site ($n = 0.94 \pm 0.16$) with a dissociation constant of 7.3 ± 0.6 μM, corresponding to a free energy of binding of about 3 kcal/mol. From the data in Figure 7 we cannot determine whether there are additional binding sites, since data cannot be obtained at low ratios of α-crystallin/melittin, due to the precipitation of α-crystallin under those conditions. Similar results are obtained with melittin derivatives RII7 and RII23 (data not shown).

When an α-crystallin−melittin complex of melittin RII21 is prepared with approximately 1:1 stoichiometry and the EPR spectra examined at low temperature, there is no evidence of spin−spin interaction (Figure 6e). Thus the

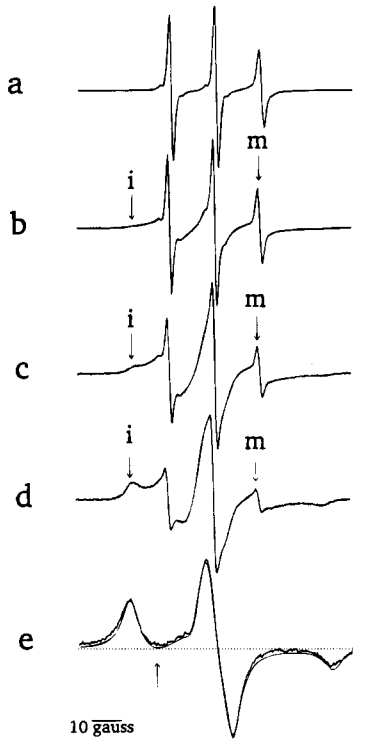

FIGURE 6: EPR spectra of spin-labeled melittin RII21 in the presence of various concentrations of α-crystallin. The molar ratios of α-crystallin monomer/melittin are (a) 0, (b) 0.5, (c) 1, and (d) 3. The mobile signal (m) is due to unbound spin-labeled melittin in solution, while the immobile signal (i) arises from melittin bound to α-crystallin. (e) Spectrum of sample from spectrum c recorded at 183 K. The light trace is the simulated spectrum in the absence of dipolar interactions between spins.

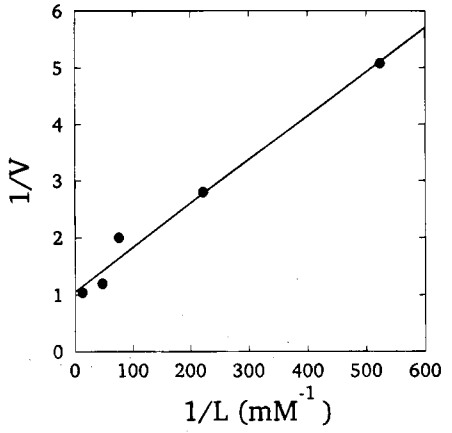

FIGURE 7: Analysis of melittin RII21−α-crystallin equilibrium binding data. Samples of labeled melittin (1.5 μL of a 0.35 mM solution) were added to different concentrations of α-crystallin in 20 mM Tris buffer, pH 7.9 (molar ratios α-crystallin/melittin, 0.25:1 to 8:1). The concentrations of free melittin (L) and bound melittin were determined from the EPR spectra as described under Methods. From the known amounts of α-crystallin in the sample, V = (bound melittin)/(total α-crystallin) was computed. The data were fit to the equilibrium binding isotherm $1/V = 1/n + k/(nL)$, where n is the number of independent sites and k is the dissociation constant.

bound melittin molecules are spatially separated in the complex, as in the case of bound insulin B chain.

If α-crystallin is introduced into a solution of melittin RII21 in high ionic strength (2.0 M NaCl, 100 mM phosphate buffer, pH 7.0) where melittin is predominantly tetrameric, results similar to those described above are obtained (data not shown). Thus, although the binding of melittin to

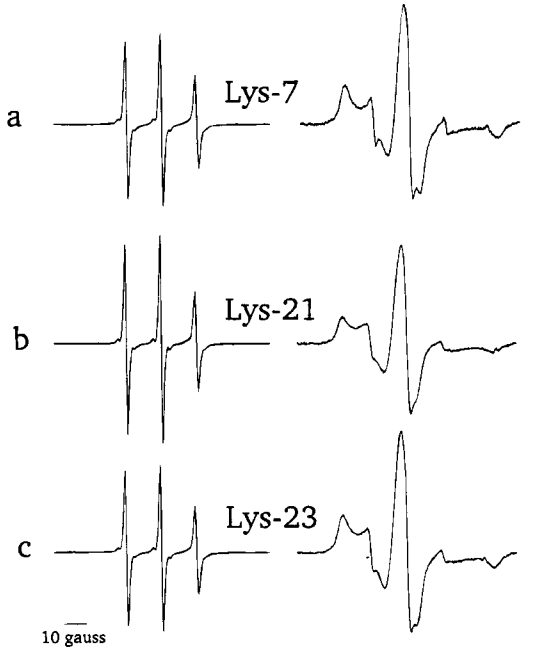

FIGURE 8: Comparision of the EPR spectra of the spin-labeled melittin derivatives RII7, RII21, and RII23 in solution and bound to an excess of α-crystallin at room temperature.

α-crystallin is relatively weak, it is sufficient to compete favorably with binding in the tetramer.

Figure 8 shows the EPR spectra in the presence of excess α-crystallin for melittin derivatives RII7, RII21, and RII23. Table 1 gives the values for A_{zz}, A_{zz}' and τ for each of the derivatives bound to α-crystallin. In addition, the A_{zz} values for the derivatives in a 20% glycerol−water glass at 183 K without α-crystallin are provided for comparison and are very similar to those for the bound protein. As for the insulin derivatives, the nitroxides are in an immobilized state in a polar environment.

In the probable situation that the exchange rate between bound and free melittin is slow compared to the electron spin−lattice relaxation rate of the bound species, the accessibility of the nitroxide in the complex can be ascertained by determining $\Pi(O_2)$ in equilibrium with air. The values for melittins RII7, RII21, and RII23 are 0.02, 0.06, and 0.07, respectively. Comparing with the reference values given earlier, it may be concluded that RII7 is inaccessible, while RII21 and RII23 are sufficiently accessible to be exposed to bulk solvent.

DISCUSSION

In the general meaning of the term, α-crystallin fulfills the definition of a molecular chaperon by being able to recognize and bind to unfolded domains of proteins and to prevent nonspecific aggregation without interacting with the native state (Hendrick & Hartl, 1993; Ellis & van der Vies, 1991; Getting & Sambrook, 1992). The mode of interaction of unfolded proteins with chaperons is a subject of current interest, and the results presented above focus on the interaction with simple peptides, the B chain of insulin and the melittin monomer, with a putative chaperon available in large quantities, α-crystallin. An important feature of these systems is that the interaction of the peptides with α-crystallin can be studied under conditions which do not affect the stability of α-crystallin itself. In the case of insulin,

unfolding can be triggered by the reduction of the two interchain disulfides. Since α-crystallin has no disulfide bonds, it is unaffected by the reduction. For melittin, the random coil is the stable state under the conditions used here, and the interaction with α-crystallin can be directly investigated.

The results presented above on insulin demonstrate that α-crystallin prevents the aggregation of the B chain by the formation of a stable complex. Due to the insolubility of the B chain, no attempt was made to investigate the equilibrium binding properties. However, the stability of the complex during isolation on gel permeation chromatography suggests a insignificant dissociation constant. Although a molar ratio of α-crystallin monomer/insulin B chain of 1.7:1 completely prevents aggregation of the B chain (Figure 1), this stoichiometry may be determined by the kinetics of the process and does not necessarily reflect an equilibrium binding stoichiometry.

Analysis of the spectral line shapes in the frozen state show that, for one B chain per 1.7 monomers of α-crystallin, the B chains are not clustered together on the surface of the protein but are bound to distinct sites such that the interspin distances between the nitroxides in adjacent chains are ≥25 Å. For the B chain derivative RI(7,19) bearing two spin labels, dipolar interaction between the two nitroxides was observed, and the interspin distance was estimated to be 20 ± 5 Å. In the native fold, the interspin spacing would be 21 ± 2 Å, based on the crystal structure of insulin and modeling of the nitroxide side chain. In a random coil configuration, the average interspin distance can be estimated to be about 32 Å (Cantor & Schimmel, 1980). Thus the B chain in the complex is folded in a fashion that brings the nitroxides closer together than in a random coil and similar to the distance in the native fold. However, the estimated width of the distribution may mean that the fold is not unique.

The B chain in the complex appears to be strongly immobilized along much of its length, as judged by the 30–50-ns correlation times of the RI(7,19) and RII29 derivatives. The same is true for melittins RII7, RII21, and RII23, all with correlations times of approximately 30 ns. For comparison, the computed rotational correlation time for the α-crystallin oligomer (800 kDa) is 200 ns. Thus the nitroxides on the bound protein have a motion faster than that expected on the basis of rotational motion of the entire complex. This may be due to independent rotations of the monomer in the complex and/or from motions of the nitroxides relative to the monomers.

The nitroxides in insulin B RI(7,19) are relatively inaccessible to collision with O_2, suggesting buried sites. However, these residues must have some degree of accessibility to solution since the cysteines in the complex react readily with spin label (I). In addition, the values of A_{zz} for insulins B RI(7,19) and B RII29 indicate a polar environment in the binding site, suggesting a degree of solvent exposure, although this could possibly arise from hydrogen bonding of the nitroxide to groups on the protein. For melittins RII7, RII21, and RII23, A_{zz} indicates a polar site in the complex. For RII21 and RII23, the relatively high accessibility to collision with O_2 suggests solvent exposed sites on the surface of the complex.

Melittin monomers are known to hydrophobically bind to membrane surfaces (Altenbach & Hubbell, 1988) and other proteins (O'Neil & DeGrado, 1990; Laine et al., 1988). The binding induces the formation of an α-helix in melittin, since only in this configuation are the hydrophobic residues properly aligned to form an interaction surface. If this simple mode of binding applied to the interaction of melittin and α-crystallin, one would expect spin labels at RII7 and RII21 to be mobile in the bound state, since they are located at the polar, noninteracting surface of the amphipathic melittin helix (Figure 5). However, the nitroxide in each spin-labeled derivative of melittin investigated is strongly immobilized by the interaction with α-crystallin, suggesting a different mode of association. The mobility data are not inconsistent with a melittin helix completely buried within the α-crystallin structure or with a β strand conformation for melittin with residues 7, 21, and 23 on the same surface.

Equilibrium binding data suggest a stoichiometry of 1 melittin per α-crystallin monomer with a dissociation constant of approximately 7.3 μM. As mentioned, data at high ratios of melittin to α-crystallin could not be obtained, and additional binding sites with larger dissociation constants would not be revealed by the data in Figure 7. The binding of melittin to α-crystallin is apparently weak compared to the B chain of insulin, although the peptides are of similar length. The 1:1 binding stoichiometry of melittin/α-crystallin monomer is an average stoichiometry and cannot be used to distinguish between a uniform distribution of one melittin on each monomer and nonuniform distributions such as two melittins on $^1/_2$ of the monomers, three melittins on $^1/_3$ of the monomers, and so forth. A uniform distribution of binding sites in the complex would be expected for the rhombic dodecahedral model of Wistow (1993), in which each monomer is chemically equivalent. Nonuniform distributions could arise from physically nonequivalent positions of the monomers in the structure, such as in the three-layered models of Tardieu et al. (1986). Thus, the average stoichiometry does not provide a means of distinquishing these models.

With the highest affinity sites saturated with melittin, no dipolar interactions were detected between nitroxides, indicating that the average interspin distance is ≥25 Å. If each subunit of α-crystallin has an equivalent binding site exposed on the surface of the complex, the average interspin distance would be ≈30 Å, assuming a spherical shape for the complex with a radius of 61 Å (Boyle et al., 1993). This corresponds approximately to the model of Wistow (1993) and is consistent with the >25 Å limit estimated experimentally. In a three-layer model, approximatelly $^1/_3$ of the subunits are located in the external layer (Tardieu, 1986; Bindels et al., 1979). If one assumes that only the outermost layer is available for melittin binding, each subunit would be required to bind three melittin molecules with equal affinities. In this case, the maximum interspin distance between nitroxides on one subunit could still exceed 25 Å if the three sites are distributed on the surface of a spherical subunit of radius 18 Å. Thus, more information is needed to distinguish between these models.

The site-directed spin-labeling method (SDSL) has been shown to be a viable approach for mapping topography and determining secondary structure in proteins (Hubbell & Altenbach, 1994). Future experiments using SDSL with both synthetic peptides and proteins should permit the secondary structure of the bound species to be determined. In addition, the binding region in the α-crystallin can be mapped using site-directed spin labels on α-crystallin itself.

REFERENCES

Adamska, I., & Kloppstech, K. (1991) *Eur. J. Biochem. 198*, 375−381.

Altenbach, C., & Hubbell, W. L. (1988) *Proteins: Struct., Funct., Genet. 3*, 230−242.

Altenbach, C., Marti, T., Khorana, H. G., & Hubbell, W. L. (1990) *Science 248*, 1088−1092

Altenbach, C., Greenhalgh, D. A., Khorana, H. G., & Hubbell, W. L. (1994) *Proc. Natl. Acad. Sci. U.S.A. 91*, 1667−1671.

Augusteyn, R. C., & Koretz, J. F. (1987) *FEBS Lett. 222*, 1−5.

Augusteyn, R. C., Parkhill, E. M., & Stevens, A. (1992) *Exp. Eye Res. 54*, 219−228.

Bhat, S. P., & Nagineni, C. N. (1989) *Biochem. Biophys. Res. Commun. 158, 319−325.*

Bhat, S. P., Nagineni, C. N., Horwitz, J., & Tom, D. (1988) *Invest. Ophthalmol. Vis. Sci. 29*, 426.

Bindels, J. G., Siezen, R. J., & Hoenders, H. J. (1979) *Ophthalmic Res. 11*, 441−452.

Bloemendal, H., Ed. (1981) in *Molecular and Cell Biology of the Eye Lens*, John Wiley, New York.

Blomendal, H., & de Jong, W. W. (1991) in *Progress in Nucleic Acid Research and Molecular Biology* (Cohen, W. E., & Moldave, K., Eds.) Vol. 41, pp 259−281, Academic Press, San Diego.

Bloemendal, H., Berbers, G. A. M., de Jong, W. W., Ramaekers, F. C. S., Vermorken, A. J. M., Dunia, I., & Benedetti, E. L. (1984) in *Human Cataract Foundation, Ciba Foundation Symposium 106,* pp 177−186, Pitman, London.

Boyle, D., Gapalakrishnan, S., & Takemoto, L. (1993) *Biochem. Biophys. Res. Commun. 192*, 1147−1154.

Cantor, C. R., & Schimmel, P. R., Eds. (1980) *Biophysical Chemistry*, W. H. Freeman and Company, New York.

Chepelinsky, A. B., King, C. R., & Zelenka, P. S. (1985) *Proc. Natl. Acad. Sci. U.S.A. 82*, 2334−2338.

Dasgupta, S., Hohman, T. C., & Carper, D. (1992) *Exp. Eye Res. 54*, 461−470.

Dubin, R. A., Wawrousek, E. F., & Piatigorsky, J. (1989) *Mol. Cell. Biol. 9*, 1083−1091.

Ellis, R. J., & van der Vies, S. M. (1991) *Annu. Rev. Biochem. 60*, 321−347.

Farahbakhsh, Z. T., Altenbach, C., & Hubbell, W. L. (1992) *Photochem. Photobiol. 56*, 1019−1033.

Gaestel, M., Schroder, W., Benndorf, R., Lippmann, C., Buchner, K., Hucho, F., Erdmann, V. A., & Bielka, H. (1991) *J. Biol. Chem. 266*, 14721−14724.

Getting, M. J., & Sambrook, J. (1992) *Nature 335*, 33−45.

Goldman, S. A., Bruno, G. V., & Freed, J. H. (1972) *J. Chem. Phys. 59*, 3071−3091.

Griffith, O. H., Dehlinger, P. J., & Van, S. P. (1974) *J. Membr. Biol. 15*, 159−192.

Harding, J. J., & Crabbe, M. J. C. (1984) in *The Eye* (Davson, H., Ed.) Vol. 1B, pp 207−492, Academic Press, New York.

Hendrick, J. P., & Hartl, F. U. (1993) *Annu. Rev. Biochem. 62*, 349−384.

Horwitz, J. (1992) *Proc. Natl. Acad. Sci. U.S.A. 89*, 10449−10453.

Hubbell, W. L., & Altenbach, C. (1994) *Curr. Opin. Struct. Biol. 4*, 566−573.

Hubbell, W. L., Froncisz, W., & Hyde, J. S. (1987) *Rev. Sci. Instrum. 58*, 1879−1886.

Inaguma, Y., Shinohara, H., Goto, S., & Kato, K. (1992) *Biochem. Biophys. Res. Commun. 182*, 844−850.

Ingolia, T. D., & Graig, E. A. (1982) *Proc. Natl. Acad. Sci. U.S.A. 79*, 2360−2364.

Iwaki, T., Kume-Iwaki, A., Liem, R. K. H., & Goldman, J. E. (1989) *Cell 57*, 71−78.

Jakob, U., & Buchner, J. (1994) *Trends Biochem. Sci. 19*, 205−211.

Jakob, U., Gaestel, M., Engel, K., & Buchner, J. (1993) *J. Biol. Chem. 268*, 1517−1520.

Kantorow, M., & Piatigorsky, J. (1994) *Proc. Natl. Acad. Sci. U.S.A. 91*, 3112−3116.

Kato, K., Shinohara, H., Kurobe, N., Goto, S., Inaguma, Y., & Oshima, K. (1991) *Biochim. Biophys. Acta 1080*, 173−180.

Klemenz, R., Frohli, E., Steiger, R., Schafer, R., & Aoyama, A. (1991) *Proc. Natl. Acad. Sci. U.S.A. 88*, 3652−3656.

Knauer, B. R., & Napier, J. J. (1976) *J. Am. Chem. Soc. 98*, 4395−4400.

Laine, R. O., Morgan, P., & Esser, A. F. (1988) *Biochemistry 27*, 5308−5314.

Landry, J., Lambert, H., Zhou, M., Lavoie, J. N., Hickey, E., Weber L. A., & Anserson, C. W. (1992) *J. Biol. Chem. 267*, 794−803.

Lowe, J., Landon, M., Pike, I., Spendlove, I., McDermott, H., & Mayer, R. J. (1990) *Lancet 336*, 515−516.

Merck, K. B., Groenen, P. J. T. A., Voorter, C. E. M., De Haard-Hoekman, W. A., Horwitz, J., Bloemendal, H., & de Jong, W. W. (1993) *J. Biol. Chem. 268*, 1046−1052.

Miron T., Vancompernolle, K., Vanderkerchhove, J., Wilchek, M., & Geiger, B. (1991) *J. Cell Biol. 114*, 255−261.

Mulders J. W. M., Wojcik, E., Bloemendal, H., & de Jong, W. W. (1989) *Exp. Eye Res. 49*, 149−152.

Nene, V., Dunne, D. W., Johnson, K. S., Taylor, D. W., & Cordinley, J. S. (1986) *Mol. Biochem. Parasitol. 21*, 179−188.

Nicholl, I. D., & Quinlan, R. A. (1994) *EMBO J. 13*, 945−953.

O'Neil, K. T., & DeGrado, W. F. (1990) *Trends Biochem. Sci. 15*, 59−64.

Overbeek, P. A., Chepelinsky, A. B., & Khillan, J. S., et al. (1985) *Proc. Natl. Acad. Sci. U.S.A. 82*, 7815−7819.

Piatigorsky, J. (1992) *J. Biol. Chem. 267*, 4277−4280.

Rao, P. V., Horwitz, J., & Zigler, J. S. (1993) *Biochem. Biophys. Res. Commun. 190*, 786−793.

Rao, P. V., Horwitz, J., & Zigler, J. S. (1994) *J. Biol. Chem. 269*, 13266−13272.

Resek, J., Farahbakhsh, Z. T., Hubbell, W. L., & Khorana, H. G. (1993) *Biochemistry 32*, 12025−12032.

Sanger, F. (1949) *Biochem. J. 44*, 126−128.

Schneider, D. J., & Freed, J. H. (1989) in *Biological Magnetic Resonance* (Berliner, L. J., & Reben, J., Eds.) Vol. *8*, pp 1−76. Plenum Press, New York.

Steinhoff, H. J. (1988) *Biochem. Biophys. Methods 17*, 237−248.

Steinhoff, H. J., Dombrowsky, O., Karim, C., & Schneiderhahn, C. (1991) *Eur. Biophys. J. 20*, 293−303.

Tardieu, A., Laporte, D., Licinio, P., Krop, B., & Delaye, M. (1986) *J. Mol. Biol. 192*, 711−724.

Terwilliger, T. C., & Eisenberg, D. (1982) *J. Biol. Chem. 257*, 6010−6015.

Thomson, J. A., & Augusteyn, R. C. (1984) *J. Biol. Chem. 259*, 4339−4345.

Teitze, F., Mortimore, G. E., & Lomax, N. R. (1962) *Biochim. Biophys. Acta 59*, 336−346.

Walsh, M. T., Sen, A. C., & Chakrabarti, B. (1991) *J. Biol. Chem. 266*, 20079−20084.

Wilcox, W., & Eisenberg, D. (1992) *Protein Sci. 1*, 641−653.

Windle, J. J. (1981) *J. Magn. Reson. 45*, 432−439.

Wistow, G J. (1993) *Exp. Eye Res. 56*, 729−732.

Wistow, G. J., & Piatigorsky, J. (1988) *Annu. Rev. Biochem. 57*, 479−504.

BI941728T